

Supplemental information

Optogenetic activation of striatal D1R and D2R

cells differentially engages downstream

connected areas beyond the basal ganglia

Christina Grimm, Stefan Frässle, Céline Steger, Lukas von Ziegler, Oliver Sturman, Noam Shemesh, Daria Peleg-Raibstein, Denis Burdakov, Johannes Bohacek, Klaas Enno Stephan, Daniel Razansky, Nicole Wenderoth, and Valerio Zerbi

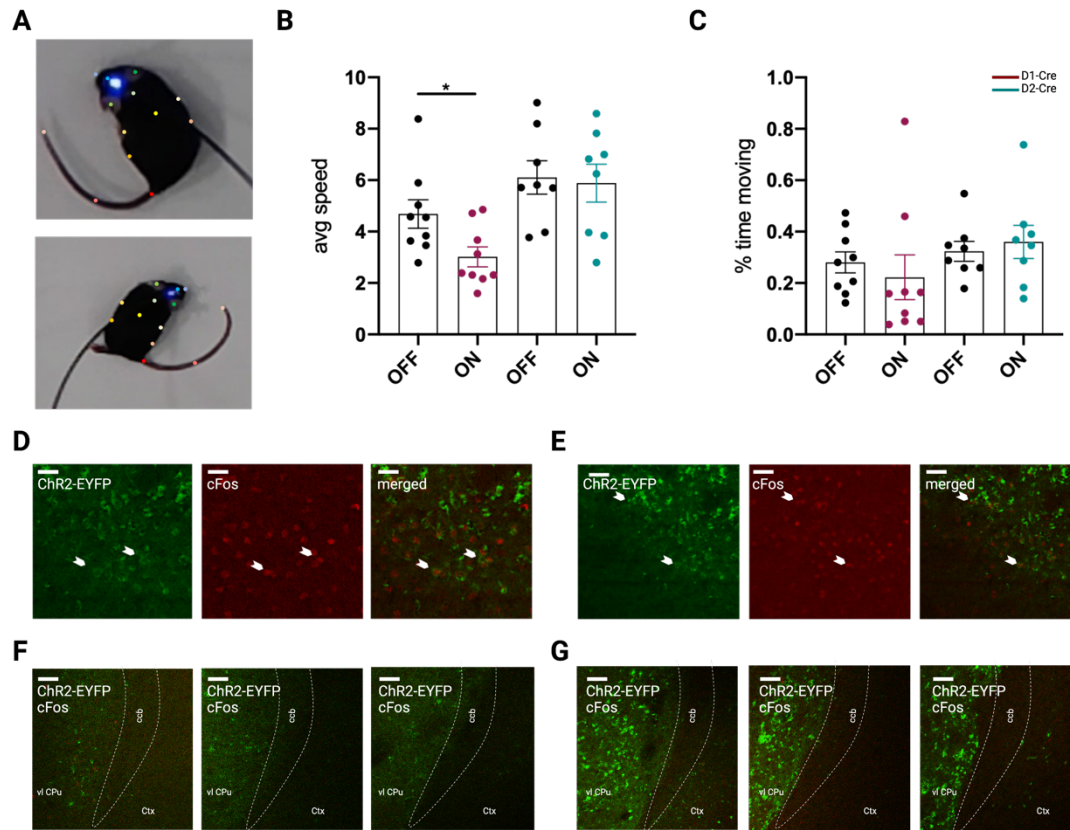


Figure S1 Optogenetic stimulation of striatal D1R and D2R cells elicits changes at the behavioural and molecular level. Related to Figure 1. **A** Position of 13 body point labels for pose estimation using DeepLabCut. **B** Optogenetically evoked motor behaviour measured as changes in average speed. In D1-Cre mice, optogenetic stimulation significantly decreases average speed (* $p = 0.03$, linear mixed effects model with post hoc test), while no stimulation effect was detected in D2-Cre mice ($p = 0.97$, linear mixed effects model with post hoc test). **C** Optogenetically evoked motor behaviour measured as changes in percent of time moving. During optogenetic stimulation of striatal D1R and D2R cells no changes in the percent of time moving were detected ($p(D1) = 0.55$, $p(D2) = 0.64$, linear mixed effects model with post hoc test). **D** Histological verification of ChR2 and cFos expression 90 min after sustained laser stimulation in vl CPu D1R cells. White arrowheads indicate representative cells co-expressing ChR2-EYFP and the stained antibody cFos. **E** Histological verification of ChR2 and cFos expression 90 min after sustained laser stimulation in vl CPu D2R cells. White arrowheads indicate representative cells co-expressing ChR2-EYFP and the stained antibody cFos. **F** Quantification of cFos expression in ChR2-EYFP D1-Cre mice. **G** Histological assessment of ChR2 and cFos expression in adjacent cortical region of D1-Cre mice. **H** Histological assessment of ChR2 and cFos expression in adjacent cortical region of D2-Cre mice. VI CPu, ventrolateral caudate putamen; ccb, corpus callosum, body; ctx, cortex. ** $p < 0.01$, *** $p < 0.001$. Scale bars, 50 μ m, 100 μ m.

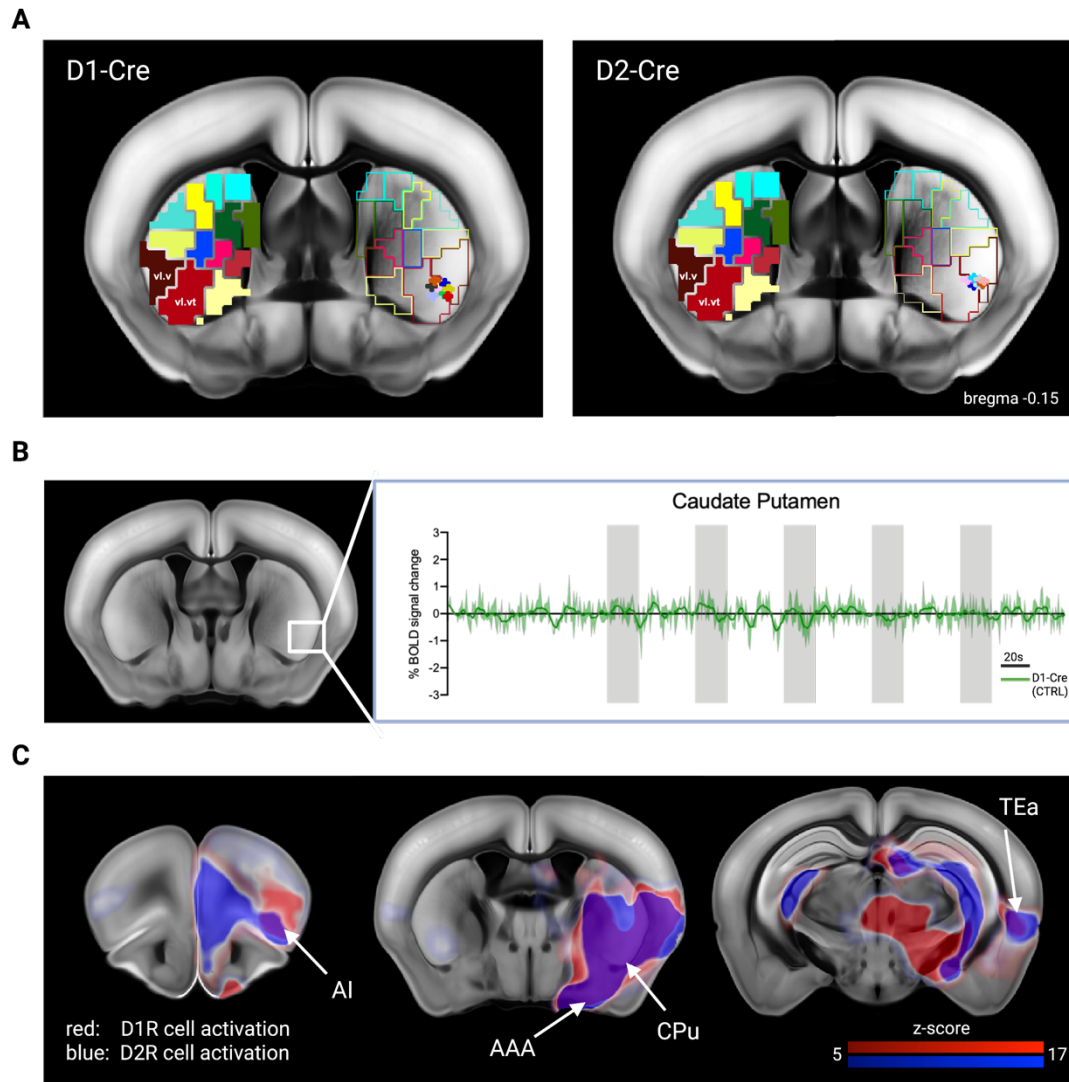


Figure S2 Optogenetic stimulation of D1R and D2R cells in the ventrolateral CPu drives brain-wide activation and de-activation hotspots. Related to Figure 2. **A** Anatomical MRI verification of optical fiber placement in the vl CPu sub-region of D1- and D2-Cre mice. **B** Mean time-series extracted from the right vl CPu of control animals depicted in green ($n(\text{D1}) = 3$ animals; no opsin expression). Laser stimulation blocks indicated in grey. **C** Overlay of thresholded D1 and D2 group z-stat activation maps, showing brain regions of similar BOLD signal profile. D1-Cre group z-stat activation map displayed in red color code, D2-Cre group z-stat activation map displayed in blue color code. $N(\text{D1-Cre})=11$, $n(\text{D2-Cre})=8$. Vl.v, ventrolateral-ventral; vl.vt, ventrolateral-ventral tip; AI, agranular insula; CPu, caudate putamen; AAA, anterior amygdalar area; TEa, temporal association area.

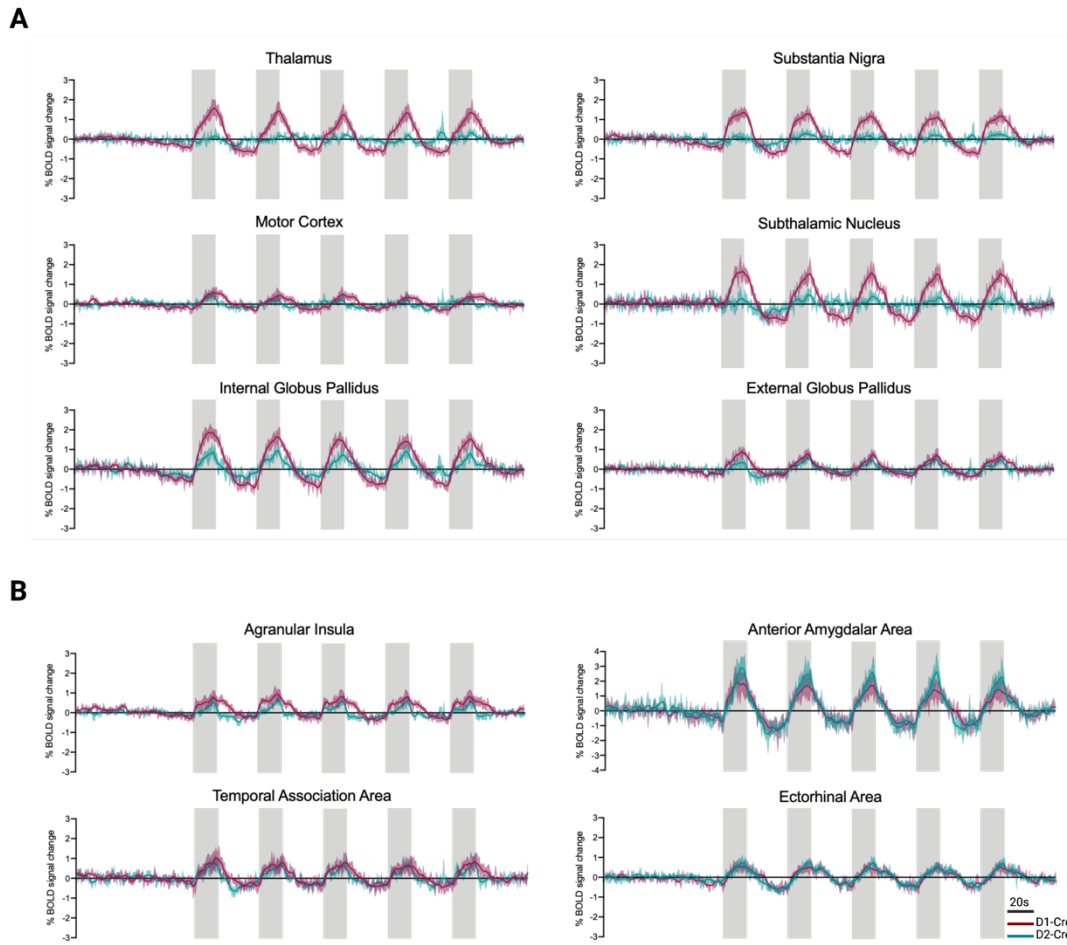


Figure S3 Mean time-series of GE BOLD local activation maxima and minima. Related to Figure 2. **A** Mean time-series of D1-/D2-Cre mice extracted from selected BG regions of interest based on GE BOLD local activation maxima and minima z-stat maps. **B** Mean time-series of D1-/D2-Cre mice extracted from selected extra-BG regions of interest based on GE BOLD local activation maxima and minima z-stat maps. D1-Cre time-series depicted in maroon, D2-Cre time-series depicted in teal. Laser stimulation blocks indicated in grey. $N(\text{D1-Cre})=11$, $n(\text{D2-Cre})=8$.

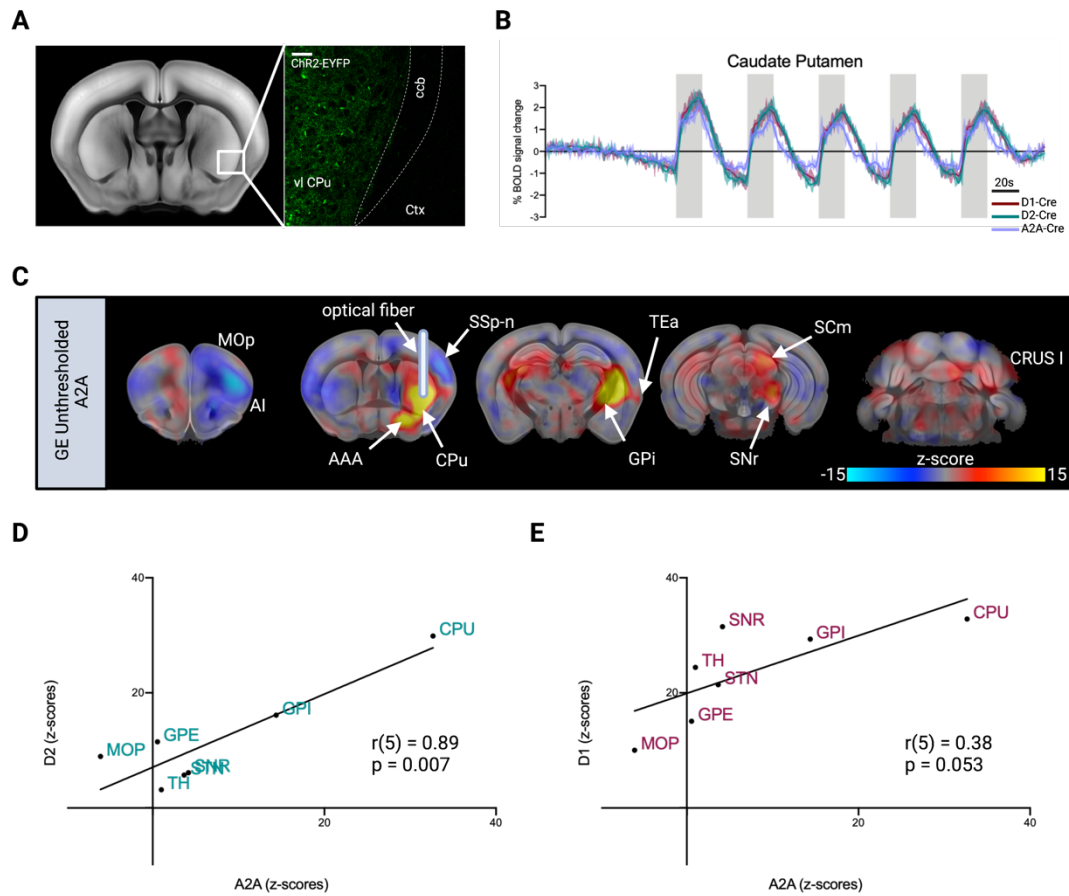


Figure S4 D2 MSN stimulation elicits distinct BOLD signal changes. Related to Figure 2. **A** Viral targeting of ChR2-EYFP to the vl CPU in A2A-Cre mice and **B** overlay of mean time-series of D1-/D2-/A2A-Cre mice extracted from vl CPU. **C** Unthresholded GLM z-stat activation maps of D2 MSN stimulation. **D** Correlation of D2-Cre and A2A-Cre z-scores of key regions connected to the BG (Pearson's $r(5)=0.89$, $p=0.007$). **E** Correlation of D1-Cre and A2A-Cre z-scores of key regions connected to the BG (Pearson's $r(5)=0.38$, $p=0.053$). D1-Cre time-series depicted in maroon, D2-Cre time-series depicted in teal, A2A-Cre time-series depicted in lilac. Laser stimulation blocks indicated in grey. MOp, primary motor cortex; AI, agranular insula; AAA, anterior amygdalar area; CPU, caudate putamen; SSp-n, primary somatosensory area, nose; TEa, temporal association area; GPi, internal globus pallidus; SCm, superior colliculus, motor related; Crus I; GPe, external globus pallidus; TH, thalamus; STN, subthalamic nucleus; ccb, corpus callosum, body; ctx, cortex. Scale bars, 100 μ m. N(A2A-Cre)=11, n(D2-Cre)=8.

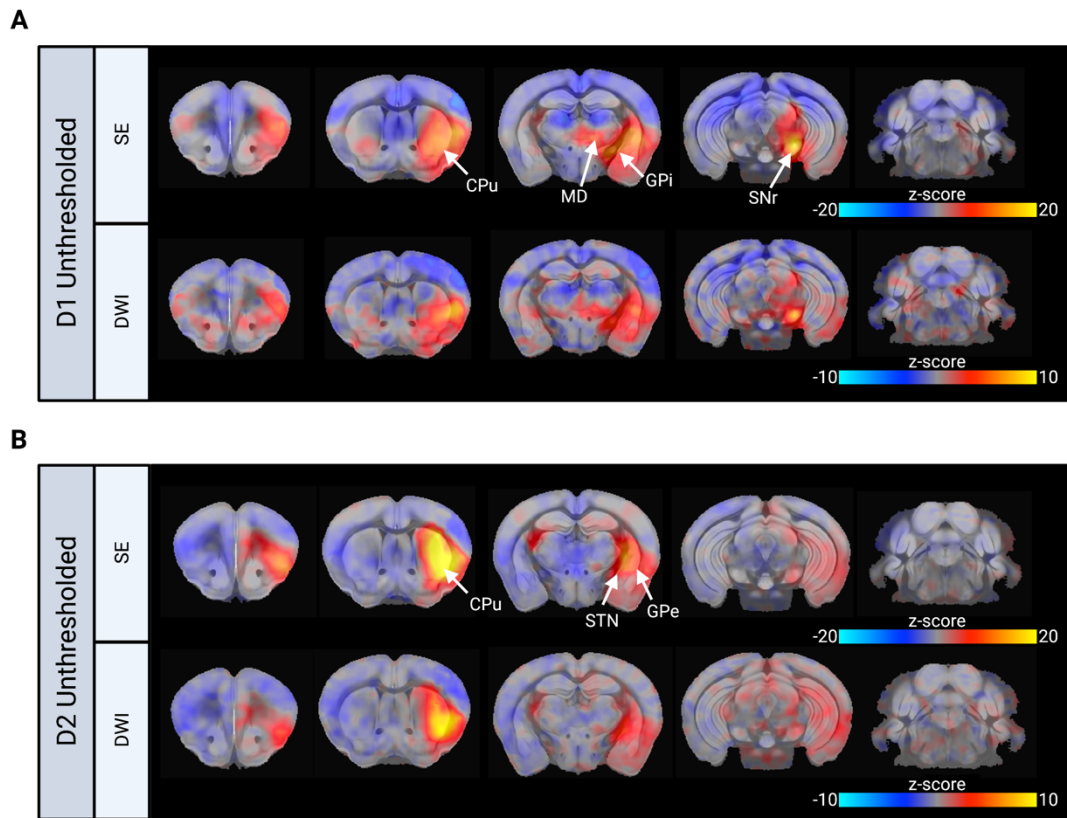


Figure S5 SE and dfMRI faithfully recapitulate causal influences of D1R and D2R cell activity within the BG. Related to Figure 2. **A** Unthresholded GLM spin-echo (SE) and dfMRI z-stat activation maps of D1R cell stimulation. **B** Unthresholded GLM SE and dfMRI z-stat activation maps of D2R cell stimulation. $N(\text{D1-Cre})=11$, $n(\text{D2-Cre})=8$. CPU, caudate putamen; GPe, external globus pallidus; GPi, internal globus pallidus; MD, mediodorsal nucleus of thalamus; STN, subthalamic nucleus; SNr, substantia nigra.

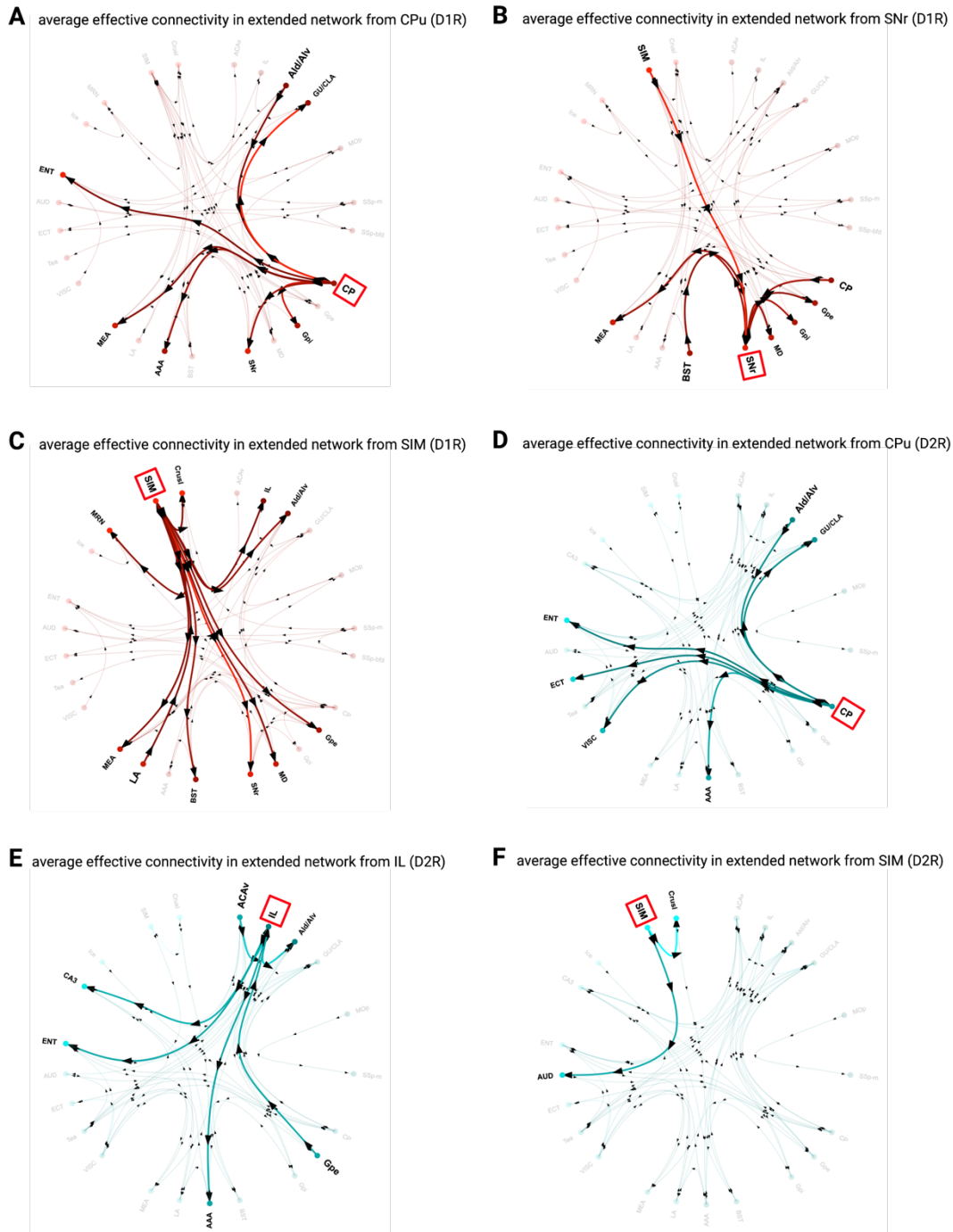


Figure S6 Maximally and minimally co-activated brain regions upon D1R and D2R cell activation. Related to STAR Methods, rDCM analysis. ACAv, anterior cingulate; IL, infralimbic area; Ald/Alv, agranular insula dorsal/ventral; MOp, primary motor cortex; SSp-m, primary somatosensory cortex, mouth area; SSp-bfd, primary somatosensory cortex, barrel field; GU/CLA, gustatory area/claustrium; CPu, caudate putamen; BST, bed nucleus of tria terminalis; AAA, anterior amygdalar area; GPe, external globus pallidus; GPi, internal globus pallidus; SBPV, subparaventricular zone; SSp-II, primary somatosensory cortex, lower limb; VISC, visceral area; TEa, temporal association area; MD, mediodorsal nucleus of thalamus; LA, lateral amygdalar nucleus; MEA, medial amygdalar nucleus; TU, tuberal nucleus; ECT, ectorhinal area; AUD, auditory area; SNr, substantia nigra; Mmme, medial mammillary nucleus, median part; CA3, cornu ammonis 3; ENT, entorhinal area; ICe, inferior colliculus, external nucleus; MRN, midbrain reticular nucleus; SIM, simple lobule; Crus I.

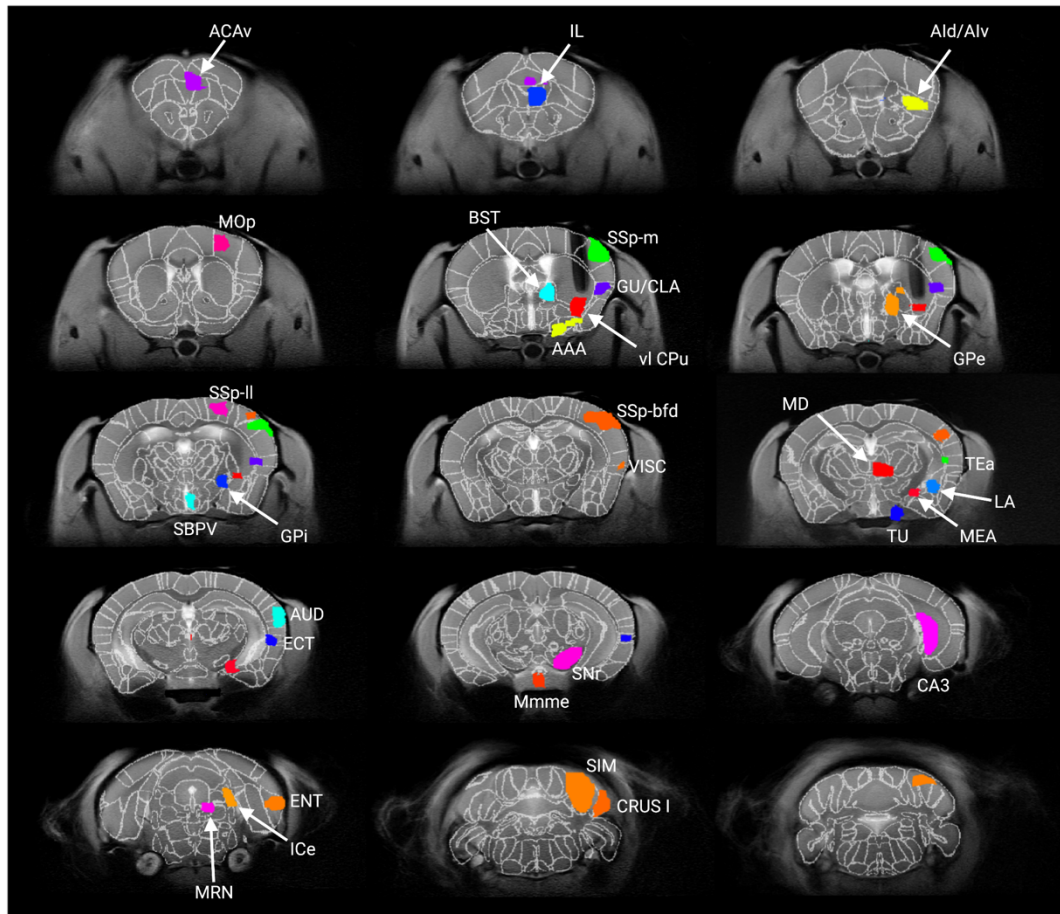


Figure S7 Whole-brain effective connectivity during D1R and D2R cell stimulation as inferred using regression DCM (rDCM). Related to Figure 5. **A** Average connectivity patterns in the extended network during D1R cell stimulation, from the CPu, **B** from the SNr, and **C** from the SIM ($P_p > 0.95$). **D** Average connectivity patterns in the extended network during D2R cell stimulation, from the IL, and **E** from the SIM ($P_p > 0.95$). Note, circo plots have been adjusted to show 50th percentile of increased directed connections only. $N(\text{D1-Cre})=11$, $n(\text{D2-Cre})=8$. AAA, anterior amygdalar area; ACAv, anterior cingulate; PrL, prelimbic area; Alv, ventral agranular insula; AUD, auditory area; BST, Bed nuclei of the stria terminalis; CA3, Ammon's horn field 3; CPu, caudate putamen; ECT, ectorhinal area; ENT, entorhinal area; GPe, external globus pallidus; GPi, internal globus pallidus; GU/CLA, gustatory area/claustrium; Ice, inferior colliculus; IL, infralimbic area; LA, lateral amygdala nucleus; MEA, medial amygdala nucleus; MD, mediodorsal nucleus of thalamus; Mmme, medial part of the medial mammillary nucleus; MOp, primary motor cortex; MRN, midbrain reticular nucleus; SIM, simple lobule; SNr, substantia nigra pars reticulata; SBPV, subparaventricular zone; SSp-bfd, primary somatosensory cortex, barrel field; SSp-II, primary somatosensory cortex, lower limb area; SSp-m, primary somatosensory cortex, mouth area; TEa, temporal association area; TU, tuberal nucleus; VISC, visceral area; Crus I.